Electronic structure and transport properties of quantum rings in a magnetic field

Jian-Bai Xia* and Shu-Shen Li
Chinese Center of Advanced Science and Technology (World Laboratory), P.O.Box 8730, Beijing 100080, China and Institute of Semiconductors, Chinese Academy of Sciences, P. O. Box 912, Beijing 100083, P. R. China
(Received 26 February 2002; published 9 July 2002)

The electronic structure of quantum rings is studied in the framework of the effective-mass theory and the two dimensional hard wall approximation. In cases of both the absence and presence of a magnetic field the electron momenta of confined states and the Coulomb energies of two electrons are given as functions of the angular momentum, inner radius, and magnetic-field strength. By comparing with experiments it is found that the width of the real confinement potential is 14 nm, much smaller than the phenomenal width. The Coulomb energy of two electrons is calculated as 11.1 meV. The quantum waveguide transport properties of Aharonov-Bohm (AB) rings are studied complementarily, and it is found that the correspondence of the positions of resonant peaks in AB rings and the momentum of confined states in closed rings is good for thin rings, representing a type of resonant tunneling.

DOI: 10.1103/PhysRevB.66.035311 PACS number(s): 73.21.Fg, 71.35.−y, 77.84.Bw, 81.05.Ea

I. INTRODUCTION

In the past few years, self-assembled dots have attracted considerable interest because their atomlike properties make them a good venue for studying the physics of confined carriers and many-body effects. They could also lead to interesting device applications in fields such as quantum cryptography, quantum computing, optics, and optoelectronics. Altering growth conditions Garcia *et al.*[1] fabricated quantum dots with a ring shape. The decisive difference between quantum rings and quantum dots is their topology—the hole in their middle becomes dominant when an external magnetic field is applied. The magnetic flux that penetrates the interior of the ring will then determine the nature of the electronic states. Warburton *et al.*[2] reported how the optical emission (photoluminescence) of a single ring changes abruptly whenever an electron is added to the ring, and that the sizes of the jumps reveal a shell structure. Lorke *et al.*[3] employed capacitance spectroscopy and infrared absorption spectroscopy to investigate both the ground states and excitations of these rings. Applying a magnetic field perpendicular to the plane of the rings, they found that, when an on-flux quantum threads the interior of each ring, a change in the ground state from angular momentum $m=0$ to $m=-1$ takes place. Theoretically, Llorens *et al.*[4] studied the electronic states of quantum rings under an applied lateral electric field. Li and Xia[5] calculated the electronic and hole states of the InAs/GaAs quantum rings of different shapes.

In this paper we study the electronic states of quantum rings in perpendicular magnetic field and transport properties of corresponding Aharonov-Bohm (AB) rings. Ignoring the effects of spins and the mutual interactions, we calculate the Coulomb energy of two electrons. We must point out that our approach is really a single particle picture, which can be useful as a first step for a more deep study of transport properties in quantum rings. At a low free-electron density, the single-particle picture is a good approximation.

Because the height of typical rings (2 nm) is much smaller than their lateral size (60 and 140 nm in outer diameter, and 20 nm in internal diameter),[3] we can use an adiabatic approximation where the motion along the z axis is decoupled from that in the xy plane, and we only consider the confined states in the xy plane.

II. THEORETICAL MODEL

In the presence of a magnetic field the equation of the radial movement of electrons in the ring is written as

$$\frac{\hbar^2}{2m^*}\left[-\frac{\partial^2\phi}{\partial r^2}-\frac{1}{r}\frac{\partial\phi}{\partial r}+\frac{m^2}{r^2}\phi+\frac{1}{\hbar^2}\left(\beta\hbar m+\frac{\beta^2}{4}r^2\right)\phi\right]+V(r)\phi=E\phi, \tag{1}$$

where m^* is the effective mass of electron, m is the angular momentum quantum number, $\beta=eB/c$, and $V(r)$ is the radial confinement potential,

$$V(r)=\begin{cases}0, & r_1\leqslant r\leqslant r_2\\ \infty, & r<r_1, r>r_2;\end{cases} \tag{2}$$

here we use the hard wall approximation, r_1 and r_2 are the inner and outer radius of the ring, respectively.

In the following we use the width of ring $d=r_2-r_1$ as the length unit, and the transverse confinement energy of the ground state,

$$E_0=\frac{\hbar^2}{2m^*}\left(\frac{\pi}{d}\right)^2, \tag{3}$$

as the energy unit. Equation (1) can be written as a dimensionless form

$$-\frac{\partial^2\phi}{\partial r^2}-\frac{1}{r}\frac{\partial\phi}{\partial r}+\frac{m^2}{r^2}\phi+\left(\frac{\pi}{2}mb+\frac{\pi^4}{16}b^2r^2\right)\phi+V(r)\phi=\pi^2E\phi, \tag{4}$$

where b is the magnetic field strength of dimensionless form:

 ©2002 The American Physical Society

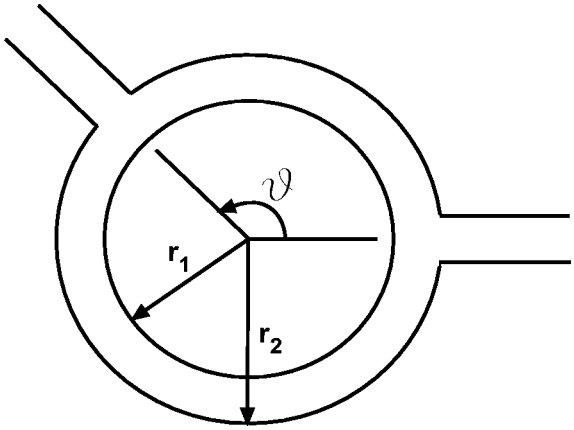

FIG. 1. Schematic illustration of the Ahanorov-Bohm ring.

$$b=\frac{\hbar eB}{\frac{m^*c}{E_0}}. \tag{5}$$

We use

$$\psi_n=\sqrt{\frac{2}{r}}\sin n\pi(r-r_1) \tag{6}$$

as the basic function, and the matrix elements of the kinetic energy terms in Eq. (4) can be represented by the sine-integral si(u) and cosine-integral ci(u).[6]

The Coulomb energy of two electrons or the binding energy of exciton state can be calculated by

$$E_c=\frac{e^2}{\varepsilon_0}\int r_i dr_i|\phi_i(r_i)|^2\int r_j dr_j|\phi_j(r_j)|^2 \times\frac{1}{2\pi}\int\frac{d\theta}{[r_i^2+r_j^2-2r_ir_j\cos\theta]^{1/2}} =\frac{2e^2}{\pi\varepsilon_0}\int_{r_1}^{r_2}r_i dr_i|\phi_i(r_i)|^2\int_{r_1}^{r_2}r_j dr_j|\phi_j(r_j)|^2\frac{1}{\sqrt{r_i+r_j}}K(r), \tag{7}$$

where ε_0 is the static dielectric constant, ϕ_i and ϕ_j are wave functions of two carriers, and $K(r)$ is the complete elliptic integral of first kind:[6]

$$r=\frac{4r_ir_j}{r_i^2+r_j^2+2r_ir_j}. \tag{8}$$

Because the transmission extreme of an AB ring is connected with the quasiconfined states,[7] we can study its transport properties to obtain the information of electronic states in corresponding closed ring. The AB ring is schematically illustrated in Fig. 1, where the central region is the ring; the electron wave is injected and partly reflected in the channel at the right ($\theta=0$), and it partly runs out in the channel at the θ angle.

The wave function in the channel region can be written as

$$\psi_c=\sum_{l=1}^{N}(a_le^{ik_lx}+b_le^{-ik_lx})\phi_l(y), \tag{9}$$

where x is the coordinate along the channel outward from the ring region, and y is the transverse coordinate. $\phi_l(y)$ is the transverse confined state with energy E_l, and N is the number of transverse modes involved in the transport:

$$\phi_l(y)=\sqrt{2}\sin l\pi y, \qquad E_l=l^2. \tag{10}$$

Note that here we use d and E_0 as the length and energy units, respectively. k_l is the propagation wave vector for the lth tranverse mode (in units of $1/d$),

$$k_l=\pi\sqrt{E-E_l}, \tag{11}$$

where E is the electron total energy, and k_l may be real or imaginary.

The wave function in the ring region can be written as

$$\psi_r=\frac{1}{\sqrt{2\pi}}\sum_{m=-M}^{M}c_m\phi_m(kr)e^{im\theta}, \tag{12}$$

where $\phi_m(kr)$ is the radial wave function for the angular momentum m and energy E, which satisfies the boundary condition $\phi_m(kr_1)=0$, and $k=\pi\sqrt{E}$. In the absence of a magnetic field,

$$\phi_m(kr)=J_m(kr)+\alpha_mY_m(kr), \tag{13}$$

where $J_m(kr)$ and $Y_m(kr)$ are the Bessel functions of first and second kinds, respectively. In the presence of magnetic field $\phi_m(kr)$ is a degenerate hypergeometric function, which is calculated by numerical integration.

By using the boundary conditions to be satisfied by the wave functions at the interface between the channel and the ring region (if we neglect the difference between the straight line of the channel and the arc line of the ring), we obtain a set of equations of coefficients a_l and b_l and a_l' and b_l' in wave function (9) for $\theta=0$ and θ channels, respectively, and c_m in the wave function (12) (Ref. 7):

$$\sum_{l=1}^{N}(a_l+b_l)I_{-ml}+\sum_{l=1}^{N}(a_l'+b_l')I'_{-ml}=c_m\phi_m(kr_2), \qquad m=0,\pm1,\pm2,\ldots\pm M, \tag{14}$$

$$ik_n(a_n-b_n)=k\sum_{m=0}^{M}c_m\phi_m'(kr_2)I_{mn}, \quad n=1,2,\ldots N, \tag{15}$$

$$ik_n(a_n'-b_n')=k\sum_{m=0}^{M}c_m\phi_m'(kr_2)I'_{mn}, \quad n=1,2,\ldots N \tag{16}$$

where

$$I_{mn}=\sqrt{\frac{r_2}{\pi d}}\int_{\theta_1}^{\theta_2}\sin\frac{n\pi r_2(\theta-\theta_1)}{d}e^{im\theta}d\theta,$$
$$I'_{mn}=\sqrt{\frac{r_2}{\pi d}}\int_{\theta_3}^{\theta_4}\sin\frac{n\pi r_2(\theta-\theta_3)}{d}e^{im\theta}d\theta. \quad (17)$$

θ_1 and θ_2 and θ_3 and θ_4 are angles to which the two sides of the two channels correspond, respectively.

There are $2M+1$ radial functions involved in the summation of Eq. (12), and N transverse states involved in the summation of Eq. (9); then we obtain $2M+2N+1$ equations. In Eqs. (14)–(16) b_n and b'_n are coefficients of electron waves traveling inward or increasing exponentially with x (for imaginary k_n), which are all set to be zero according to physical consideration, except one coefficient $b_i=1/\sqrt{k_i}$, representing the amplitude of one injected wave. There are $2M+2N+1$ unknown coefficients in Eqs. (14)–(16): $a_n, a'_n (n=1,2,\ldots N)$ and $c_m (m=0,\pm1,\ldots\pm M)$; therefore the set of equations is complete and unique.

Solving the set of equations we obtain the coefficients a_n and a'_n, which are related to the transmission and reflection amplitudes

$$a_n=\frac{r_{ni}}{\sqrt{k_n}},$$
$$a'_n=\frac{t_{ni}}{\sqrt{k_n}}. \quad (18)$$

The total transmission and reflection probabilities are given by

$$T=\sum_{ij}|t_{ij}|^2,$$
$$R=\sum_{ij}|r_{ij}|^2. \quad (19)$$

III. RESULTS AND DISCUSSION

A. Effect of curvature

In the following we use the electron momentum $\kappa=\sqrt{E}$ to represent the energy E (in units of E_0). In the special case of a straight two-dimensional wire of width d, the transverse energy is $E_l=l^2$, and the electron momentum is $\kappa=l$, i.e., an integer. In the absence of magnetic field Fig. 2 shows the κ as functions of the angular momentum m for a ring of $r_1=0.25$, which corresponds to a typical ring,[3] with an inner radius of 10 nm and an outer radius of 50 nm in the length unit of the ring width $d=40$ nm. From Fig. 2 we see that for $m=0$ κ is nearly equal to and smaller than an integer n ($n=1,2,\ldots$), which is caused by the curvature of the ring. When $r_1\to\infty$, the ring approaches the wire limit, and all κ's approach n. When $r_1\to0$, the ring approaches the circle limit, and κ of the m state approaches α_m^n/π, where α_m^n is the nth zero point of the Bessel function of mth order $J_m(x)$. For example, for $m=0$, $\kappa=0.7655$, 1.7571, 2.7546, 3.7535, . . . , $m=1$, $\kappa=1.2197$, 2.2446, 3.2382, 4.2412, . . . , etc.

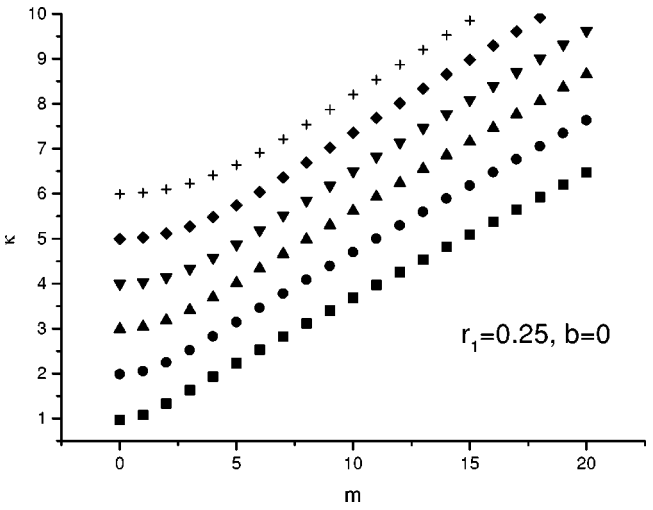

FIG. 2. Electron momentum as a function of the angular momentum m for a ring of $r_1=0.25$ in $b=0$.

B. Effect of magnetic field

In the presence of a magnetic field Fig. 3 shows κ's as functions of m for the magnetic field $b=4$ and the ring of $r_1=0.25$. For a typical ring[3] $d=40$ nm, $m^*=0.07m_0$, the energy unit $E_0=3.36$ meV [Eq. (3)]. $b=4$ [Eq. (5)] corresponds to $B=8.12$ T. From Fig. 3 we see that the energy minimum is at $m<0$ state, which is caused by the mb linear term in Eq. (4). The absolute value of m, at which the energy minimum is located, increases when the magnetic field b increases or the inner radius r_1 increases, due to increase of the magnetic flux through the ring.

Figure 4 shows κ's of the ground state and the first excited state ($n=1,2$) as functions of b for $m=0$, -1, and -2 states. From Fig. 4 we see that when the magnetic field

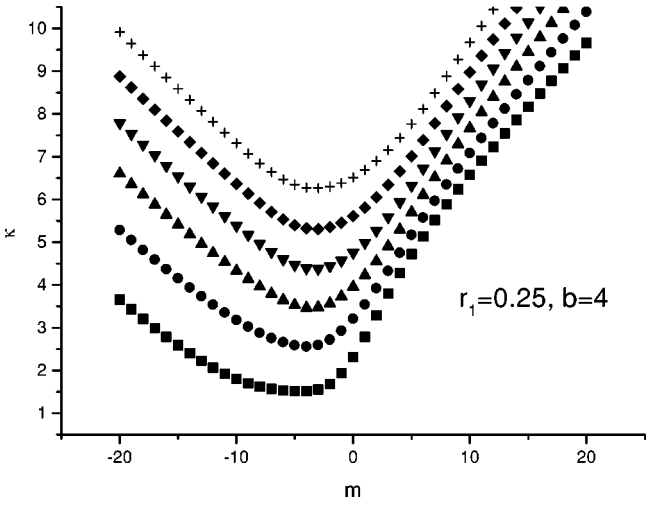

FIG. 3. Electron momentum as a function of the angular momentum m for a ring of $r_1=0.25$ in $b=4$.

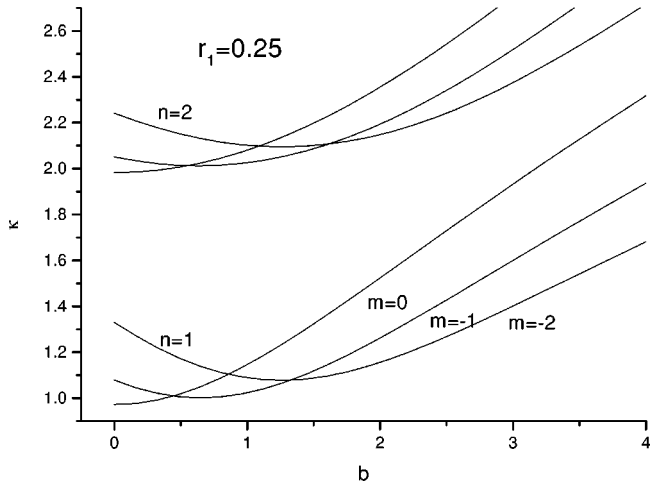

FIG. 4. Electron momentum as a function of the magnetic-field strength b for the $m=0$, 1, and 2 states of a ring of $r_1=0.25$.

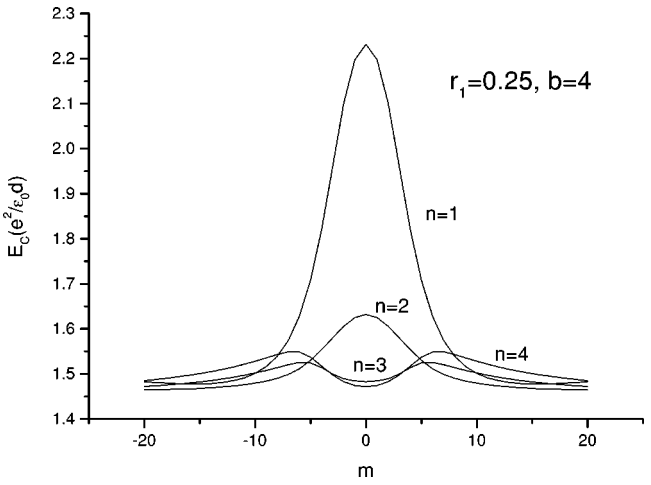

FIG. 6. Coulomb energies of two electrons as functions of the angular momentum m for a ring of $r_1=0.25$ in $b=4$.

increases the ground state changes gradually from an $m=0$ state to $m=-1,-2,\ldots$ states. There is an abrupt change of energy at the transition of m, which occurs at $b=0.5$ for the transition from the $m=0$ state to the $m=-1$ state. This is verified by the experiment,[3] where it was found that the transition occurs at $B=8$ T. From $b=0.5$ and $B=8$ T we obtain the real ring width $d=14$ nm; this means that the width of the real confinement potential is much smaller than the phenomenal width 40 nm.

C. Coulomb energy of two electrons

Figure 5 shows the Coulomb energies of two electrons as functions of m for the ring of $r_1=0.25$ in the absence of a magnetic field. The unit of the Coulomb energy is $e^2/\varepsilon_0 d$, proportional inversely to the width of ring. From Fig. 5 we see that for the $m=0$ state the Coulomb energy of the ground state is at a maximum; it then follows those of the $n=2,3,4,\ldots$ states. But for $m>5$ the order is reversed. The Coulomb energies decrease when the inner radius increases and the width is kept constant. For example, the Coulomb energies of the $m=0$ ground state are 1.6381, 1.3057, and 0.9499 $(e^2/\varepsilon_0 d)$ for $r_1=0.25$, 0.5, and 1, respectively. When r_1 is smaller, the electron density is distributed more concentratedly, resulting in increase of the Coulomb energy. There are only experimental results for the Coulomb energy of two electrons in the quantum dots,[8] which is equal to 20 meV. Another photoluminescence experiment[2] gave the binding energy of a single charged exciton (X^{1-}, two electrons plus one hole) as 6.0 meV in the ring. We assume that the width of the ring is 14 nm, from our calculation results $E_c=1.6382$ $(e^2/\varepsilon_0 d)$ and $\varepsilon_0=15.15$, we obtain $E_c=11.1$ meV, which is comparable to that in the quantum dot, and larger than the binding energy of X^{1-}.

Figure 6 shows the Coulomb energies as functions of m for the ring of $r_1=0.25$ in the magnetic-field $b=4$. From Fig. 6 we see that the Coulomb energies are larger than those in the absence of magnetic field, due to the $\pi^2 b^2 r^2/16$ term of the magnetic field potential in Eq. (4), the electrons are distributed more closely to the central region. The Coulomb energies are symmetric with respect to $m=0$ state, different from the eigenenergies in Fig. 3. From Eq. (4) we see that

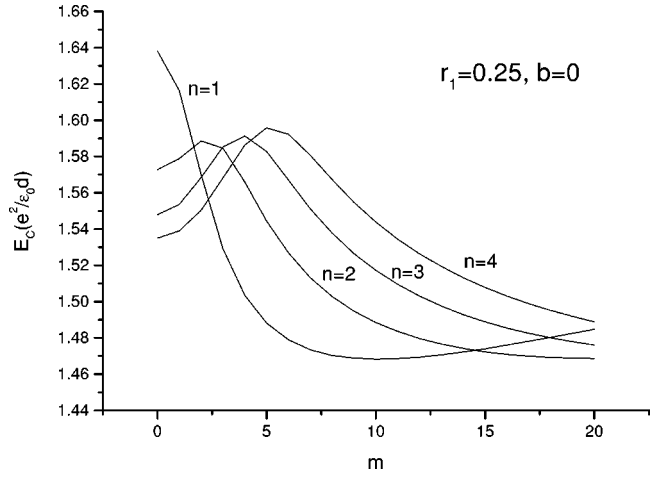

FIG. 5. Coulomb energies of two electrons as functions of angular momentum m for a ring of $r_1=0.25$ in $b=0$.

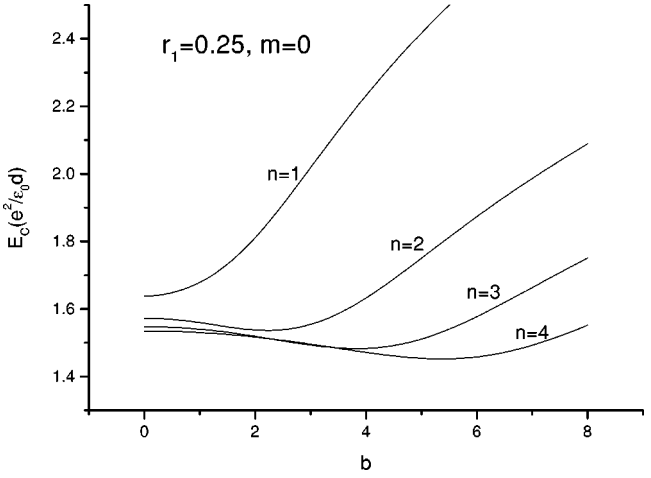

FIG. 7. Coulomb energies of two electrons as functions of the magnetic-field strength b for the $m=0$ state of a ring of $r_1=0.25$.

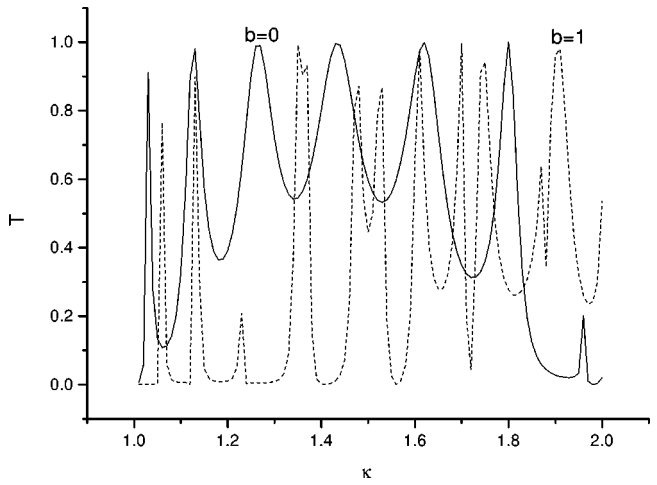

FIG. 8. Transmission probabilities as functions of the electron momentum for an AB ring of $r_1=1$ and $\theta=\pi$ in $b=0$ (solid line) and $b=1$ (dashed line).

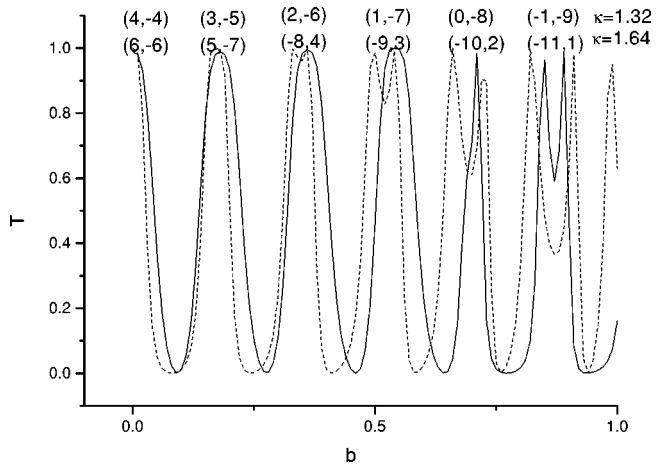

FIG. 9. Transmission probabilities as functions of the magnetic-field strength b for the electron momenta $\kappa=1.32$ (solid line) and 1.62 (dashed line) in an AB ring of $r_1=1$ and $\theta=\pi$.

the $\pi mb/2$ term is a constant, only changes the eigenenergy, and has no effect on the wave function.

Figure 7 shows the Coulomb energies of the $m=0$ state as functions of the magnetic field b for the ring of $r_1=0.25$. From Fig. 7 we see that when the magnetic field increases the Coulomb energy of the ground state increases; however those of excited states decrease first, then increase as b becomes larger than a critical value. The above results are all suitable for the exciton states composed of electron and hole states.

D. Mesoscopic transport properties

For a thin ring ($r_1 \geqslant 1$) we can investigate the quantum waveguide transport properties of an AB ring to obtain information about the confined states in the corresponding ring. Figure 8 shows the transmission probabilities T as functions of the momentum of injected electron for an AB ring of $r_1=1$ and $\theta=\pi$ (see Fig. 1) in both $b=0$ and 1. From Fig. 8 we see that there is a series of resonant peaks, corresponding to the momentum of confined states in the closed ring with different angular momentum m. Tables I and II gives the positions of resonant peaks and momentum κ of the ring, and corresponding m. From Tables I and II we see that the consistency is good in the case of either zero or finite magnetic field, so we can use the AB ring to investigate the energy spectra of a closed ring.

Figure 9 shows the transmission probabilities as functions of a magnetic field b for an AB ring of $r_1=1$, $\theta=\pi$, and electron momentum $\kappa=1.32$ and 1.62. From Fig. 9 we see that T changes periodically with magnetic field, which is the basic characteristic of the AB ring.[9,10] The oscillating period is

$$\Phi=\frac{hc}{e}, \tag{20}$$

where Φ is the magnetic flux through the ring section area. Assuming that the ring has an average radius r_0, we obtain the period represented by b:

$$b=\frac{4}{(\pi r_0)^2}, \tag{21}$$

From Fig. 9 the oscillating period is $b=0.18$, then we obtain $r_0=1.50$, just as the average radius for the ring of $r_1=1$ and $r_2=2$. The figures in Fig. 9 represent the angular momentum m of corresponding states in the closed ring. At $b=0$, the peaks of two curves correspond to $m=\pm 4$ and ± 6 states, respectively. When b increases, each peak corresponds to $m-1$ states related to the former peak. They are split into two peaks at b near to 1, which is also in agreement with the calculation results of confined states in the closed ring. To our knowledge is a new type of resonant tunneling that occurs in the plane structure without the barrier region, in contrast to that in a double-barrier quantum-well structure.

For fat rings ($r_1<1$) the correspondence is not good, because the two channels have a large part of boundary with the ring, and have influence on the confined states (see Fig. 1).

TABLE I. Positions of resonant peaks in the AB ring, and momenta of confined states in a closed ring in $b=0$.

AB ring	κ	1.03	1.13	1.27	1.44	1.62	1.80	1.96
closed ring	m	2	3	4	5	6	7	8
	κ	1.08	1.18	1.31	1.46	1.62	1.79	1.96

IV. SUMMARY

The electronic structure of quantum rings is studied in the framework of the effective-mass theory and the two dimensional hard wall approximation. In the absence of a magnetic field the electron momentum κ of the $m=0$ state is nearly equal to an integer n (transverse momentum), and approaches α_m^n/π for the m state as the inner radius r_1 approaches zero. In the presence of magnetic field, the ground

TABLE II. Positions of resonant peaks in the AB ring and momenta of confined states in a closed ring in $b=1$.

AB ring	κ	1.06	1.13	1.23	1.23	1.35	1.37	1.48	1.53	1.61	1.70	1.75	1.87	1.91
closed ring	m	-4	-3	-2	-9	-1	-10	-11	0	-12	1	-13	2	-14
	κ	1.08	1.15	1.25	1.27	1.39	1.39	1.52	1.54	1.65	1.71	1.79	1.89	1.94

state is at $m<0$ state, and the $|m|$ value is dependent on the magnetic-field strength b and the inner radius r_1. When the magnetic field increases, the ground state will change gradually from an $m=0$ state to $m=-1,-2,\ldots$ states. The Coulomb energy of the ground states of two electrons increases with increasing magnetic field. By comparing with experiments it is found that the width of the real confinement potential is about 14 nm, much smaller than the phenomenal width. Using this width the Coulomb energy of the two electrons in the ring is obtained as 11.1 meV, which is comparable to that in the quantum dot. The quantum waveguide transport properties of AB rings are studied complementarally, it is found that the correspondence of the positions of resonant peaks in AB rings and the momentum of confined states in closed rings is good for thin rings ($r_1 \geqslant 1$), representing a type of resonant tunneling.

ACKNOWLEDGMENTS

This work was supported by the National Natural Science Foundation of China, special funds for Major State Basic Research Project No. G2001CB309500 of China, and a project of the Chinese Academy of Sciences: Nanometer Science and Technology.

*Email address: xiajb@red.semi.ac.cn

[1] J. M. Garcia, G. Medeiros-Ribeiro, K. Schmidt, T. Ngo, J. L. Feng, A. Lorke, and J. Kotthaus, Appl. Phys. Lett. **71**, 2014 (1997).

[2] R. J. Warburton, C. Schaflein, D. Haft, F. Bickel, A. Lorke, K. Karrai, J. M. Garcia, W. Schoenfeld, and P. M. Petroff, Nature (London) **405**, 926 (2000).

[3] A. Lorke, R. J. Luyken, A. O. Govorov, J. P. Kotthaus, J. M. Garcia, and P. M. Petroff, Phys. Rev. Lett. **84**, 2223 (2000).

[4] J. M. Llorens, C. Trallero-Giner, A. Garcia-Cristobal, and A. Cantarero, Phys. Rev. B **64**, 035309 (2001).

[5] S. S. Li and J. B. Xia, J. Appl. Phys. **89**, 3434 (2001); **91**, 3227 (2002).

[6] L. S. Gradshteyn and I. M. Ryzhik, in *Table of Integrals, Series, and Products* (Academic Press, New York, 1980).

[7] W. D. Sheng and J. B. Xia, J. Phys. C **8**, 3635 (1996).

[8] G. Medeiros-Ribeiro, F. G. Pikus, P. M. Petroff, and A. L. Efros, Phys. Rev. B **55**, 1568 (1997); P. M. Petroff, A. Lorke, and A. Imamoglu, Phys. Today **54** (5), 46 (2001).

[9] S. Datta and S. Bandyopadhyay, Phys. Rev. Lett. **58**, 717 (1987).

[10] J. B. Xia, Phys. Rev. B **45**, 3593 (1992).